Towards Dynamic Object Manipulation with Tactile Sensing for Prosthetic Hands

Wenceslao Shaw-Cortez, Denny Oetomo, Chris Manzie, and Peter Choong

***Abstract*— The manipulation of objects is an inherent capability of dexterous human hands. However, state-of-the-art prostheses are limited to only forming grasps and gestures due to the low information transfer rate in the human-machine interface. Additionally, in the prosthetic setting the hand is not privy to such global knowledge including the object's shape, weight, friction properties, etc. Existing techniques from robotics that can manipulate objects in this prosthetic setting require compensation terms which are counterproductive to the manipulation task. The incorporation of tactile sensing leads to a simpler control formulation and enables relaxation of several restrictive assumptions inherent in the robotics applications. In this work a novel control system is proposed that incorporates tactile sensing for object manipulation and optimal distribution of contact forces for prosthetic hands. Simulation results demonstrate the ability of the proposed control system to manipulate an object, while minimizing the use of frictional forces during manipulation.**

I. Introduction

Despite advances in technology, prosthetic hands are well behind a human hand's capabilities. The main limitation of current prostheses lies in the human-machine interface [1], [2]. Current technology can only gather a low number of signals from the user to command the prosthesis. As the hand complexity and number of degrees of freedom increases, a sophisticated interface is needed to map the few input signals to the many commands and/or tasks of the hand. Despite this limitation, many prosthetic hands have been developed to improve the quality of living of amputees. However most research is focused only on improving grasp capabilities. Little focus has been given to a key dexterous capability of human hands: manipulation.

One of the classifications of object manipulation is in-hand manipulation where an object is translated and/or rotated within a grasp [3]. With only grasp capabilities, manipulation tasks using typically available prostheses would require bulk movement of the arm. For example, to open a water bottle the user would need to form a grasp around the cap, then rotate his/her entire arm to unscrew the cap. These large motions lead to user fatigue, poor performance, and physical limitations in constrained environments that affect the quality of living for amputees [3]. Many amputees are forced to change their occupation due to the lack of dexterity in today's prosthetic technology [4]. Alternatively, in-hand manipulation exploits hand dexterity to efficiently accomplish these everyday tasks.

Current state-of-the-art prostheses are focused on solving the interface's low bandwidth problem using techniques such as finite state machines, pattern recognition, and postural synergies [5], [6]. However those approaches are mainly focused on forming gestures or grasp types without regard for grasp stability. The system becomes more complex when considering the nonlinear dynamics of a hand holding an object. An alternative approach is to embed a degree of intelligence in the prosthesis to deal with the nonlinear system as the user focuses only on task-related commands.

The robotics field has had many advances regarding grasp stability and in-hand manipulation. However many of the existing results from the robotics literature embed assumptions of known object properties that are not readily available in the context of powered prosthetic hands. One exceptional technique [7], [8] has provided a solution to stably manipulate objects without external sensing or knowledge of the object's properties. However the technique requires counterproductive control terms and conservative assumptions to avoid using external sensors. Additionally, that approach heuristically distributes the contact forces over the object, which limits the grasping capabilities of the hand.

This work proposes a novel technique that incorporates tactile sensing to enhance the prosthetic hand's capability. Existing tactile sensors and slip prevention methods [9] are used to remove unnecessary control terms and relax conservative assumptions. Additionally, the use of tactile sensing allows for a novel implementation of grasp force optimization to optimally distribute the contact forces. This work moves towards improving the quality of living of amputees by restoring the dexterous capability of manipulation on prosthetic hands.

This paper is organized as follows. Section II defines the nonlinear hand and object dynamics. Section III defines the proposed control law to provide grasp stability and manipulation for prosthetic hands. Section IV presents and discusses the results of implementing the proposed control law on a hand-object system in simulation.

II. System Dynamics

Consider a multi-fingered hand grasping a rigid, polyhedral object at k contact locations. Each finger consists of n joints with hemispherical fingertips. Let the finger configuration be defined by the joint angles, $\boldsymbol{\theta}_i \in \mathbb{R}^n$. The full hand configuration is defined by the full joint angle vector,

W. Shaw-Cortez is with the Graduate School of Mechanical Engineering, University of Melbourne, 3010, Australia, shaww@student.unimelb.edu.au.

D. Oetomo and C. Manzie are with the Department of Mechanical Engineering, University of Melbourne, 3010, Australia, {doetomo, manziec}@unimelb.edu.au.

P. Choong is with the Department of Surgery University of Melbourne, St. Vincent's Hospital, 3065, Australia, pchoong@unimelb.edu.au.

$\boldsymbol{\theta} = (\boldsymbol{\theta}_1^T, \boldsymbol{\theta}_2^T, ..., \boldsymbol{\theta}_k^T)^T \in \mathbb{R}^m$, where $m = nk$. Let the inertial frame, $\mathcal{P}$, be fixed on the palm of the hand, and let each finger i have a finger base frame, $\mathcal{S}_i$, and a fingertip frame, $\mathcal{F}_i$, located at the position $\boldsymbol{p_{f_i}} \in \mathbb{R}^3$ as shown in Figure 1.

The motion of the joints is related to the fingertip motion by the spatial Jacobian, $J_{s_i}(\boldsymbol{\theta}_i) \in \mathbb{R}^{6\times n}$:

$$\begin{bmatrix} \boldsymbol{v}_i \\ \boldsymbol{\omega}_i \end{bmatrix} = \begin{bmatrix} J_i \\ J_{\Omega_i} \end{bmatrix} \dot{\boldsymbol{\theta}}_i = J_{s_i} \dot{\boldsymbol{\theta}}_i \tag{1}$$

where $\boldsymbol{v}_i \in \mathbb{R}^3$ is the ith fingertip translational velocity, $\boldsymbol{\omega}_i \in \mathbb{R}^3$ is the ith fingertip angular velocity, and $J_i, J_{\Omega_i} \in \mathbb{R}^{3\times n}$ are the translational and rotational components of J_{s_i}, respectively. The joint motion is related to the velocity of the ith contact point via the hand Jacobian, $J_{h_i} \in \mathbb{R}^{3\times n}$ [10]:

$$J_{h_i} = \begin{bmatrix} I_{3\times 3} & -(\boldsymbol{p_{c_{f_i}}})^\wedge \end{bmatrix} J_{s_i} \tag{2}$$

where $I_{3\times 3} \in \mathbb{R}^{3\times 3}$ is the identity matrix and $\boldsymbol{p_{c_{f_i}}} \in \mathbb{R}^3$ is the vector from ith fingertip to the ith contact point. Let $\boldsymbol{p_{c_f}}$ denote the concatenation of all contact point vectors, $\boldsymbol{p_{c_{f_i}}}$. The full hand Jacobian, $J_h \in \mathbb{R}^{3k\times m}$, is constructed by combining each J_{h_i} into a block diagonal matrix for $i = 1, ..., k$.

Each fingertip exerts a contact force on the object at contact i, denoted by $\boldsymbol{f_{c_i}} \in \mathbb{R}^3$. If expressed in the contact frame, $\mathcal{C}_i$, let $\boldsymbol{f_{c_i}} = (f_{x_i}, f_{n_i}, f_{z_i})^T$ where $f_{x_i}, f_{z_i} \in \mathbb{R}$ are the tangential components and $f_{n_i} \in \mathbb{R}$ the normal component of the contact force. Let each contact force vector be concatenated into the full contact force vector, $\boldsymbol{f_c} \in \mathbb{R}^{3k}$. The dual form of the hand jacobian, J_h^T, describes the interaction from object to hand by mapping this contact force onto the corresponding torque applied at the hand joints. The dynamics of the hand are given by [11]:

$$M_h(\boldsymbol{\theta})\ddot{\boldsymbol{\theta}} + C_h(\boldsymbol{\theta}, \dot{\boldsymbol{\theta}})\dot{\boldsymbol{\theta}} + N_h(\boldsymbol{\theta}, \dot{\boldsymbol{\theta}}) = -J_h^T \boldsymbol{f_c} + \boldsymbol{\tau} \tag{3}$$

where $M_h, C_h \in \mathbb{R}^{m\times m}$ are the respective inertia and coriolis matrices, $N_h \in \mathbb{R}^m$ represents the remaining forces such as gravity and friction that act on the joints, and $\boldsymbol{\tau} \in \mathbb{R}^m$ is the joint torque control input for a fully actuated hand.

Let the object's configuration be defined by the combined position and orientation vector, $\boldsymbol{x} \in \mathbb{R}^6$. The orientation of the object is represented by the rotation matrix, $R_{po}(\boldsymbol{x}) \in \mathbb{R}^{3\times 3}$, which maps the object frame, $\mathcal{O}$, to the inertial frame, $\mathcal{P}$. Each finger contacts the object at the respective contact point, $\boldsymbol{p_{c_i}} \in \mathbb{R}^3$, and the position vector from the object frame to said contact point is $\boldsymbol{p_{c_{o_i}}} \in \mathbb{R}^3$. A visual representation of the contact geometries between the ith finger and the object is shown in Fig. 1. Note that in this paper the i^{th} contact point refers to the origin of the $\mathcal{C}_i$ frame, and the i^{th} fingertip refers to the origin of the $\mathcal{F}_i$ frame.

The grasp map, $G_i \in \mathbf{R}^{6\times 3}$, maps the contact forces, $\boldsymbol{f_{c_i}}$, to the corresponding wrench acting on the object. The dual form of the grasp map, G_i^T, maps object motion to the velocity of the ith contact point. This grasp map can be computed by [10]:

$$G_i^T = \begin{bmatrix} I_{3\times 3} & -(\boldsymbol{p_{c_{o_i}}})^\wedge \end{bmatrix} \tag{4}$$

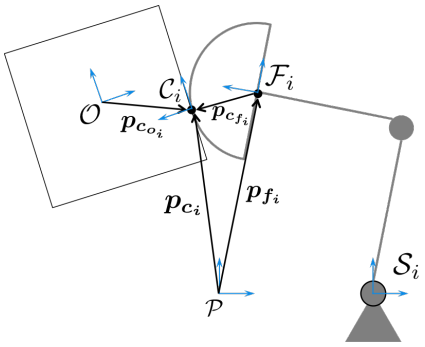

Fig. 1: A visual representation of contact geometries for contact i.

The full grasp map, $G = [G_1, G_2, ..., G_k] \in \mathbb{R}^{6\times 3k}$, maps the full contact force vector to the net object wrench. The object dynamics are given by [11]:

$$M_o(\boldsymbol{x})\ddot{\boldsymbol{x}} + C_o(\boldsymbol{x}, \dot{\boldsymbol{x}})\dot{\boldsymbol{x}} = G\boldsymbol{f_c} + \boldsymbol{w_e} \tag{5}$$

where $M_o, C_o \in \mathbb{R}^{6\times 6}$ are the object's respective inertia and coriolis matrices and $\boldsymbol{w_e} \in \mathbb{R}^6$ is an external wrench disturbing the object. The hand and object kinematics are related by the grasp constraint [11]:

$$J_h\dot{\boldsymbol{\theta}} = G^T\dot{\boldsymbol{x}} \tag{6}$$

Assuming that the contact points do not slip on the object surface, their motion is constrained by this nonholonomic rolling constraint [10].

In this work, object manipulation is defined as reaching a static object configuration, $\boldsymbol{x_d} \in \mathbb{R}^6$, where the hand-object system is not moving. Due to the constraints of the prosthetic hand, the object position and orientation are not known a priori, and so related work focuses on translating and rotating an auxiliary object position and orientation defined by the hand configuration [7], [8]. Let this auxiliary object state be represented by $\boldsymbol{x}_a \in \mathbb{R}^6$, and let $\boldsymbol{\eta} := [\dot{\boldsymbol{\theta}}^T, \dot{\boldsymbol{e}}^T, \boldsymbol{e}^T]^T$ be the hand-object state, where $\boldsymbol{e} := \boldsymbol{x_d} - \boldsymbol{x}_a$ defines the error between the auxiliary and desired object configurations. Let $\boldsymbol{\eta}^{eq} := 0$ denote the desired equilibrium point. Thus object manipulation is considered to be achieved if the following asymptotic stability condition is satisfied:

$$\boldsymbol{\eta} \to \boldsymbol{\eta}^{eq} \tag{7}$$

The goal of the control system is to determine the joint torques, $\boldsymbol{\tau}$, to guarantee (7) is satisfied. By developing such a control system, the human user can focus on commanding the desired object configuration, while the control system deals with the nonlinear complexities for grasp stability.

III. Proposed Manipulation Controller

The robotics approach from Kawamura et. al. [7], [8] provides a framework for object manipulation, but must be extended to be applicable for prosthetic hands. To avoid external sensing, that approach defines the auxiliary object position with the centroid of the fingertip positions, $\bar{\boldsymbol{p}}_{\boldsymbol{f}} \in \mathbb{R}^3$, where $\bar{\boldsymbol{p}}_{\boldsymbol{f}} = \sum_{i=1}^k \boldsymbol{p_{f_i}}/k$. The auxiliary object orientation is

defined using a virtual frame computed from the fingertip positions and is represented by the rotation matrix, $R_{po_v} \epsilon \mathbb{R}^{3\times3}$ [7]. Thus in that work, the fingertip centroid, $\bar{\boldsymbol{p}}_{\boldsymbol{f}}$, and virtual frame, R_{po_v}, define the auxiliary object configuration, $\boldsymbol{x}_a$.

The assumptions used by the robotics approach include:

Assumption 1: The object is rigid and has a convex, polyhedral shape.

Assumption 2: The hand has soft, hemispherical fingertips.

Assumption 3: No external disturbance acts on the system: $\boldsymbol{w_e} = 0, N_h = 0$.

Assumption 4: The contact points do not slip on the object surface.

Assumption 5: The hand is fully actuated and has sufficient degrees of freedom for manipulation.

The control law for the robotics approach is defined by [12]:

$$\boldsymbol{\tau} = \frac{k_f}{\sum_{i=1}^{k} r_i} \sum_{i=1}^{k} J_i^T(\bar{\boldsymbol{p}}_{\boldsymbol{f}} - \boldsymbol{p_{f_i}}) - K_c\dot{\boldsymbol{\theta}} + k_{st} \sum_{i=1}^{k} J_{\Omega_i}^T \boldsymbol{r}_{ref} + k_p \sum_{i=1}^{k} J_i^T(\boldsymbol{p_d} - \bar{\boldsymbol{p}}_{\boldsymbol{f}}) + k_o \sum_{i=1}^{k} J_{\Omega_i}^T \boldsymbol{r_d} \quad (8)$$

where $k_f \epsilon R_{>0}$ is a reference force gain, $r_i \epsilon R_{>0}$ is the radius of the ith fingertip, $K_c \epsilon \mathbb{R}^{m\times m}$ is a stabilizing matrix for feedback passivity, $k_{st} \epsilon R$ is a stabilizing gain term, $\boldsymbol{r}_{ref} \epsilon \mathbb{R}^3$ is a reference command to constrain the direction of the rolling motion, k_p and $k_o \epsilon R$ are proportional gains for manipulation, $\boldsymbol{p_d} \epsilon \mathbb{R}^3$ is the desired object position, and $\boldsymbol{r_d} \epsilon \mathbb{R}^3$ is the error vector between the desired object orientation and auxiliary orientation as defined by the virtual frame. The orientation error, $\boldsymbol{r_d}$, is related to the auxiliary and desired object orientations: $\boldsymbol{r_d} = \boldsymbol{r_x} \times \boldsymbol{r_{d_x}} + \boldsymbol{r_y} \times \boldsymbol{r_{d_y}} + \boldsymbol{r_z} \times \boldsymbol{r_{d_z}}$, where $R_{po_v} = [\boldsymbol{r_x}, \boldsymbol{r_y}, \boldsymbol{r_z}]$ and the desired orientation is $R_{po_d} = [\boldsymbol{r_{d_x}}, \boldsymbol{r_{d_y}}, \boldsymbol{r_{d_z}}]$.

Theorem 1: [12] *Under Assumptions 1-5, and given a grasp with k contact points, the control law (8) satisfies the following asymptotic stability condition:*

$$\boldsymbol{\eta} \rightarrow \boldsymbol{\eta}^{eq}, \sum_{i=1}^{k} f_{n_i} \rightarrow \left(\frac{\sum_{i=1}^{k} d_i}{\sum_{i=1}^{k} r_i}\right) k_f \quad (9)$$

where d_i is the perpendicular distance between $\boldsymbol{p_{f_i}}$ and $\bar{\boldsymbol{p}}_{\boldsymbol{f}}$ with respect to the object's surface.

As a result of avoiding external sensing, that robotics approach is dependent on the fingertip positions, $\boldsymbol{p_{f_i}}$. However as discussed in [12], this results in an induced rolling motion about the contact point. To prevent this excessive rolling, the authors implement a relative attitude constraint which is incorporated as the additional control term: $k_{st} \sum_{i=1}^{k} J_{\Omega_i}^T \boldsymbol{r}_{ref}$. Their results show this relative attitude constraint to be helpful for manipulation purposes, however the term itself adds complexity in terms of more parameters to tune and acts against the desired object motion. Additionally, Assumptions 3 and 4 are too conservative for prosthetic hands which are used in unstructured environments and exposed to disturbances. That robotics approach must be extended to account for the relaxation of these simplifying assumptions present in the existing framework.

Improvements in technology have led to new tactile sensors for robotic hands [9] that can be used to develop a novel control system from the original control law of the robotics literature. With the appropriate tactile sensors, this novel controller can be a function of the contact points, $\boldsymbol{p_{c_{f_i}}}$, instead of the fingertip positions, $\boldsymbol{p_{f_i}}$. This removes the induced rolling motion, such that the relative attitude constraint in (8) is not necessary:

$$\boldsymbol{\tau} = k_f \sum_{i=1}^{k} J_{h_i}^T(\bar{\boldsymbol{p}}_{\boldsymbol{c}} - \boldsymbol{p_{c_i}}) - K_c\dot{\boldsymbol{\theta}} + J_h^T \tilde{G}^{\dagger} K_p \begin{bmatrix} \boldsymbol{p_d} - \bar{\boldsymbol{p}}_{\boldsymbol{c}} \\ \boldsymbol{r_d} \end{bmatrix} \quad (10)$$

where $\bar{\boldsymbol{p}}_{\boldsymbol{c}}$ is the centroid position of all the contact points, $(\cdot)^{\dagger}$ refers to the pseudoinverse, and $K_p = \text{diag}([k_p, k_p, k_p, k_o, k_o, k_o]) \in \mathbb{R}^{6\times6}$ is a gain matrix formed from the previous gain terms. The hand Jacobian is computed using (2), and the grasp map from (4) is approximated by:

$$\tilde{G}_i^T = \begin{bmatrix} I_{3\times3} & -(\boldsymbol{p_{c_i}} - \bar{\boldsymbol{p}}_{\boldsymbol{c}})^{\wedge} \end{bmatrix} \quad (11)$$

In this work, the auxiliary object configuration, $\boldsymbol{x}_a$, is defined by the contact centroid, $\bar{\boldsymbol{p}}_{\boldsymbol{c}}$, and the same virtual frame, R_{po_v}, but here defined as a function of the contact positions. It is important to note that with knowledge of the fingertip geometry, the contact normal vector can be determined from the same tactile sensors. This allows for a definition of a contact frame, $\mathcal{C}_i$. It is trivial to show that $\boldsymbol{p_{c_i}}$, $\bar{\boldsymbol{p}}_{\boldsymbol{c}}$, and thus $\tilde{G}$, are functions of $\boldsymbol{\theta}$ and $\boldsymbol{p_{c_f}}$.

Note the final term of (10). In (8), the object's rotation is controlled by the fingertip's rotation through the use of $J_{\Omega_i}^T$. Now that sensors are used to determine J_h and $\tilde{G}$, the grasp constraint (6) is used instead to directly relate object motion to joint motion.

With the use of tactile sensors, slip prevention methods can be incorporated into the controller. Slip prevention works by adjusting the grasp force applied on the object until no slip is detected. It is currently implemented on prosthetic hands and provides robustness to external disturbances. Here slip prevention is incorporated into the control law by adjusting the force gain, k_f. This allows for the relaxation of Assumption 4 by replacing it with the following:

Assumption 6: The slip prevention algorithm acts sufficiently fast to regulate k_f, and prevent slip.

Alternatively, new technologies have emerged that provide sensory feedback to the human user from the prosthetic hand. If such technology is available and there is sufficient bandwidth in the interface, the gain, k_f, can be regulated by the user to adjust the applied grasp force.

The use of the grasp map leads to an additional improvement upon the robotics technique. The first term of (8) is used to drive the fingertips to the fingertip centroid position. This is to apply a squeezing force on the object to ensure the object stays within the grasp. However this is a heuristic approach to distribute the contact forces. For more than two contact points, there are infinitely many solutions to this

distribution problem. This is readily seen when considering the equilibrium condition of the hand-object dynamics:

$$G\boldsymbol{f_C} + \boldsymbol{w_e} = 0 \tag{12}$$

Recall that $G \in \mathbb{R}^{6\times 3k}$. Thus when $k > 2$, and a solution to (12) exists, the solution is not unique. With infinitely many solutions, the question then becomes how to choose an appropriate contact force distribution, $\boldsymbol{f_C}$?

A technique known as grasp force optimization [13]–[15] focuses on using optimization-in-the-loop to optimally distribute the contact forces. However that technique requires knowledge of an object's friction and weight, which are not available for prosthetic hands. A novel optimization proposed here is to distribute the contact forces without knowledge of $\boldsymbol{w_e}$ or friction properties by using grasp force optimization alongside slip prevention. The idea is to let slip prevention regulate the magnitude of "squeeze" on the object, while the optimization distributes this squeeze across the contact points. So rather than incorporating the equilibrium condition (12) in the constraints as is done in conventional grasp force optimization, the optimization here is only concerned with guaranteeing that the optimal forces, $\boldsymbol{f_C^*}$, have no effect on the object's motion. This novel optimization is defined by:

$$\begin{aligned}
\boldsymbol{f_C^*}(\boldsymbol{\theta}, \boldsymbol{p_{C_f}}) \;= \underset{\boldsymbol{f_C}}{\text{argmin}} \quad & \boldsymbol{f_C}^T W \boldsymbol{f_C} && \text{(13a)}\\
\text{subject to} \quad & \tilde{G}(\boldsymbol{\theta}, \boldsymbol{p_{C_f}})\boldsymbol{f_C} = 0, && \text{(13b)}\\
& \sum_{i=1}^{k} f_{n_i} - 1 = 0 && \text{(13c)}\\
& f_{n_i} > 0,\ \forall i = 1, ..., k && \text{(13d)}
\end{aligned}$$

where $\boldsymbol{f_C}$ is defined with respect to the contact frame, $\mathcal{C}_i$, such that $\boldsymbol{f_{C_i}} = (f_{x_i}, f_{n_i}, f_{z_i})^T \in \mathbb{R}^3$.

Constraint (13b) guarantees that the net wrench from the contact force is zero. This is important to prevent the resulting solution from affecting the motion of the manipulated object. Constraint (13c) is a normalizing term, which augments the notion that (13) is used only for contact force distribution, not for adjusting how much the hand "squeezes" the object. Constraint (13d) guarantees that contact forces can only push, not pull at the contact points. For a positive-definite matrix, W, the optimization is convex and can be solved using a quadratic programming solver. The following assumption is required to guarantee existence of the solution:

Assumption 7: There exist $k > 2$ noncollinear contact points [10].

For the proposed control law, (13) is solved in-the-loop and substituted into (10):

$$\tau = k_f J_h^T \boldsymbol{f_C^*} - K_c \dot{\boldsymbol{\theta}} + J_h^T \tilde{G}^\dagger K_p \begin{bmatrix} \boldsymbol{p_d} - \bar{\boldsymbol{p}}_{\boldsymbol{C}} \\ \boldsymbol{r_d} \end{bmatrix} \tag{14}$$

Note that in (13) $\boldsymbol{f_C^*}$ and $\tilde{G}$ are defined in the contact frame, whereas in (14) they must be rotated to the inertial $\mathcal{P}$ frame.

The benefit of incorporating this novel optimization is that by choosing an appropriate weighting, W, there is flexibility in how the contact forces are distributed. For example, by penalizing tangential forces at each contact, the resulting contact force will require less friction to grasp the object. This would reduce the need of excessive grasp force to prevent slip, thus reducing the applied force on the object. Thus in contrast to the previous robotics approach, the condition on asymptotic stability for the proposed control law is modified to include these optimal contact forces:

$$\boldsymbol{\eta} \to \boldsymbol{\eta}^{eq},\ f_{n_i} \to k_f f_{n_i}^*\ \forall i = 1, .., k \tag{15}$$

where $f_{n_i}^*$ is the normal component of the ith optimal contact force, $\boldsymbol{f_C^*}$, defined by (13).

Proposition 1: Under Assumptions 1, 2, 3, 5, 6, 7, and given an initial grasp with k contact points, positive-definite weighting matrix, W, slip prevention gain, k_f, and desired object configuration, $\boldsymbol{x_d} \in \mathbb{R}^6$, the control law defined by (14) satisfies (15).

Proof: Omitted for brevity. ■

Remark 1: Through incorporation of appropriate integral action in (14), Assumption 3 may be relaxed from Proposition 1.

IV. Results

The hand-object system consists of a three-fingered hand with nine degrees of freedom, and with rigid, hemispherical fingertips holding a cube object. Two revolute joints are located at the finger base and one revolute joint connects the two links of the finger. The links all share the same dimensions and mass properties. The hand and object properties are listed in Table I. The purpose of these simulations is to show that the proposed controller, (14), demonstrates the ability to manipulate the object, while optimally distributing the contact forces. Future work will be focused on dealing with disturbances, incorporating slip prevention, and implementing on hardware.

TABLE I: Simulation Parameters

Link length	0.3 m
Link mass	0.25 kg
Link moment of inertia	$\text{diag}([0.0077, 0.0021, 0.0021])$ kgm^2
Fingertip radius	0.06 m
Object dimensions	0.2604 m $\times$ 0.2604 m $\times$ 0.2604 m
Object mass	0.0018 kg
Object moment of inertia	$\text{diag}([0.0014, 0.0014, 0.0014])$ kgm^2
Initial θ_1	$[1.047, 0, 1.571]$ rad
Initial θ_2	$[1.047, 0, 1.571]$ rad
Initial θ_3	$[1.047, 0, 1.571]$ rad
Initial object center	$[0, 0, 0.4098]$ m
Initial R_{po_v}	$I_{3\times 3}$
k_f	10
W	$\text{diag}([10, 1, 10, 10, 1, 10, 10, 1, 10])$
K_c	$0.07 * I_{9\times 9}$
k_p	3
k_o	0.5

The simulation was performed using Matlab's ode45 integrator. The optimization (13) was solved using the quadprog() function at each iteration of the ode45 integrator. The simulation time was set to 10 seconds. The value of k_f was empirically chosen such that the contact points do not lose contact with the object. In future work k_f will be determined by slip prevention algorithms.

A. *Demonstration of Object Manipulation*

In this simulation, the hand is commanded to reach an object position of $\boldsymbol{p_d} = (-0.1, 0.2, 0.4)^T$, while maintaining the initial virtual frame orientation. The affect of external disturbances on the object and hand were ignored for this simulation. Figure 2a and Figure 2b show the initial and final grasp configurations, respectively. The plots in Figure 3 show the joint angle rates, object position trajectory, object orientation error, and contact normal forces for the resulting manipulation motion.

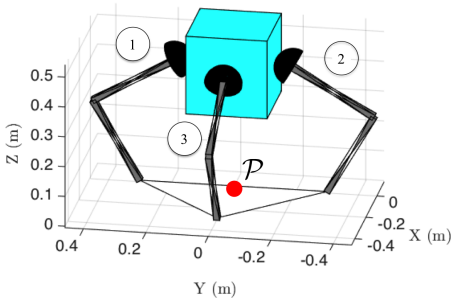

(a) Initial grasp configuration with fingers numerically labeled and the origin of the inertial palm frame, $\mathcal{P}$, depicted.

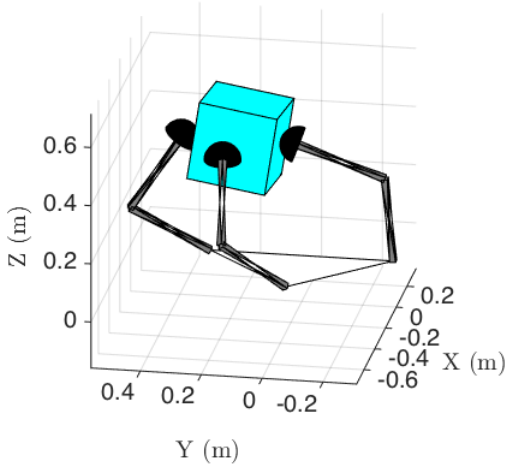

(b) Final grasp configuration.

Fig. 2: Grasp configurations of the hand-object system at initial and final times. The final auxiliary object state is defined by the position $\boldsymbol{p_d} = (-0.1, 0.2, 0.4)^T$ and the same initial R_{po_v}.

Figure 3a shows the joint angle rates converging to zero. Figure 3b shows the auxiliary object position converging to the reference position, $\boldsymbol{p_d}$. Figure 3c shows that the error between the virtual frame orientation and desired orientation, $\boldsymbol{r_d}$, converges to zero. Finally, Fig. 3d shows the normal force vectors of each contact point reaching the optimal values defined by the dashed black line. Notice however that although the normal forces reach the desired optimal values at steady state, there is some deviation from these optimal forces when the object is in motion. This deviation is a result

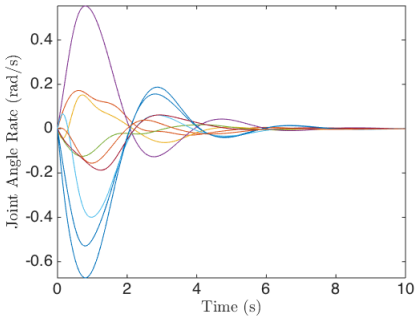

(a) Joint angle rate trajectories.

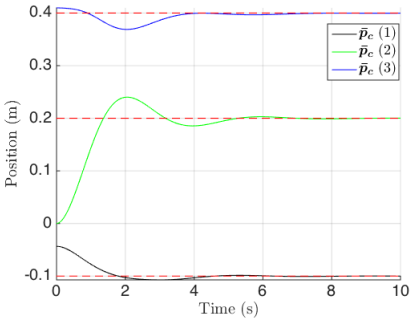

(b) Auxiliary object position trajectory.

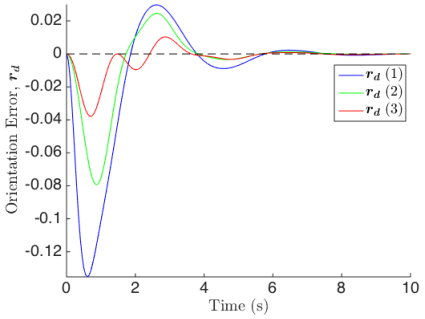

(c) Auxiliary object orientation error.

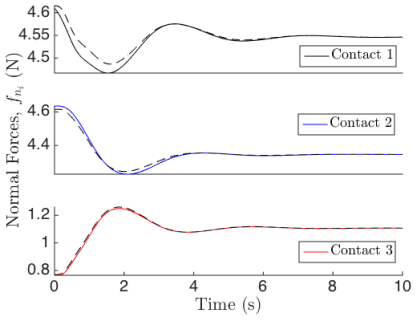

(d) Normal force trajectories.

Fig. 3: Plots of the joint angle rates, object position trajectory, and normal forces for the manipulation action. The desired equilibrium values are defined by the dashed lines. The gain values are as defined in Table I.

of the additional reaction forces from the object's motion when manipulation is performed. These figures demonstrate the ability of the proposed control law to asymptotically reach the desired equilibrium as defined in (15), thus achieving object manipulation with optimal force distribution. This also shows that the proposed controller does not require the relative attitude constraint, which adds unnecessary complexity to the original robotics control system.

B. Contact Force Distribution

A key aspect of the proposed solution is the use of the novel optimization to distribute forces in a stabilizing control framework. By careful choice of W, the optimization can be used to re-distribute contact forces by penalizing the use of tangential forces at each contact point. This results in contact forces that reduce the required friction needed to grasp the object. This can be seen by comparing the required friction coefficient for a penalized weighting, $W = \text{diag}([10, 1, 10, 10, 1, 10, 10, 1, 10])$, and a nominal weighting, $W = \text{diag}([1, 1, 1, 1, 1, 1, 1, 1, 1])$. This required friction coefficient is the ratio of tangential forces to normal forces: $\beta_i := \sqrt{f_{x_i}^2 + f_{z_i}^2}/f_{n_i}$ for $i = 1, ..., k$. The comparison between penalized and normal weights is shown in Fig. 4.

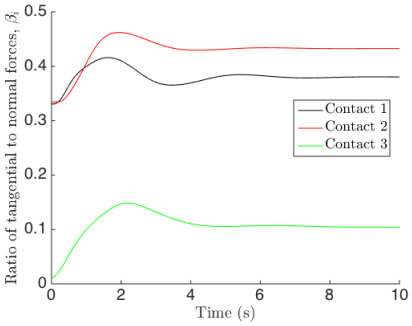

(a) Ratio of tangential to normal forces during manipulation for the nominal weighting: $W = \text{diag}([1, 1, 1, 1, 1, 1, 1, 1, 1])$

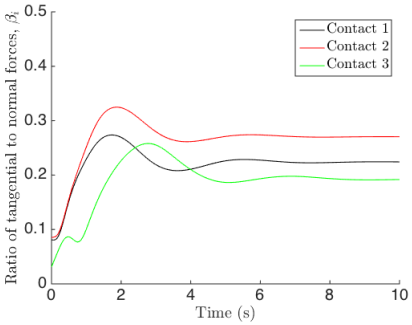

(b) Ratio of tangential to normal forces during manipulation for the penalized weighting: $W = \text{diag}([10, 1, 10, 10, 1, 10, 10, 1, 10])$

Fig. 4: A comparison of the tangential to normal force ratios for nominal and penalized weighting distributions.

The maximum β_i from the penalized weighting distribution is 0.3249, whereas that of the nominal distribution is 0.4623. The lower ratio means that the hand can grasp objects with smaller friction coefficients without slipping for the same slip gain, k_f. This prevents excess application of force when slip prevention is implemented to avoid crushing the object, and thus reduces the actuation effort of the multi-fingered hand.

V. Conclusion

In this paper a control law was proposed to provide object manipulation for prosthetic hands. The control law was modified from the existing robotics technique by incorporating tactile sensors to remove the undesired rolling motion and relax the no slip assumption. Also, a novel grasp force optimization was used in the controller to optimally distribute the contact forces. Simulation results show the ability of the of the proposed control law to manipulate an object to a desired configuration, and reduce the friction used during said manipulation.

References

[1] J. S. Schofield, K. R. Evans, J. P. Carey, and J. S. Hebert, "Applications of sensory feedback in motorized upper extremity prosthesis: a review," *Expert Review of Medical Devices*, vol. 11, no. 5, pp. 499–511, 2014.

[2] U. Wijk and I. Carlsson, "Forearm amputees' views of prosthesis use and sensory feedback," *Journal of Hand Therapy*, vol. 28, no. 3, pp. 269–278, 2015.

[3] I. M. Bullock, R. R. Ma, and A. M. Dollar, "A hand-centric classification of human and robot dexterous manipulation," *IEEE Transactions on Haptics*, vol. 6, no. 2, pp. 129–144, 2013.

[4] C. H. Jang, H. S. Yang, H. E. Yang, S. Y. Lee, J. W. Kwon, B. D. Yun, J. Y. Choi, S. N. Kim, and H. W. Jeong, "A survey on activities of daily living and occupations of upper extremity amputees," *Annals of Rehabilitation Medicine*, vol. 35, no. 6, pp. 907–921, 2011.

[5] M. Hakonen, H. Piitulainen, and A. Visala, "Current state of digital signal processing in myoelectric interfaces and related applications," *Biomedical Signal Processing and Control*, vol. 18, pp. 334–359, 2015.

[6] J. Segil and R. Weir, "Design and validation of a morphing myoelectric hand posture controller based on principal component analysis of human grasping," *IEEE Transactions on Neural Systems and Rehabilitation Engineering*, vol. 22, no. 2, pp. 249–257, 2014.

[7] K. Tahara, S. Arimoto, and M. Yoshida, "Dynamic object manipulation using a virtual frame by a triple soft-fingered robotic hand," *IEEE International Conference on Robotics and Automation*, pp. 4322–4327, 2010.

[8] A. Kawamura, K. Tahara, R. Kurazume, and T. Hasegawa, "Dynamic grasping of an arbitrary polyhedral object," *Robotica*, vol. 31, no. 4, pp. 511–523, 2013.

[9] Z. Kappassov, J. A. Corrales, and V. Perdereau, "Tactile sensing in dexterous robot hands - review," *Robotics and Autonomous Systems*, vol. 74, pp. 195–220, 2015.

[10] A. Cole, J. Hauser, and S. Sastry, "Kinematics and control of multi-fingered hands with rolling contact," *IEEE Transactions on Automatic Control*, vol. 34, no. 4, pp. 398–404, 1989.

[11] R. Murray, Z. Li, and S. Sastry, *A mathematical introduction to robotic manipulation*. CRC Press: Boca Raton, FL, USA, 1994.

[12] A. Kawamura, K. Tahara, R. Kurazume, and T. Hasegawa, "Dynamic object manipulation using a multi-fingered hand-arm system: enhancement of a grasping capability using relative attitude constraints of fingers," *International Conference on Advanced Robotics*, pp. 8–14, 2011.

[13] V. Lippiello, B. Siciliano, and L. Villani, "A grasping force optimization algorithm for multiarm robots with multifingered hands," *IEEE Transactions on Robotics*, vol. 29, no. 1, pp. 55–67, 2013.

[14] L. Han, J. C. Trinkle, and Z. X. Li, "Grasp analysis as linear matrix inequality problems," *IEEE Transactions on Robotics and Automation*, vol. 16, no. 6, pp. 663–674, 2000.

[15] A. Bicchi, "Hands for dexterous manipulation and robust grasping: a difficult road toward simplicity," *IEEE Transactions on Robotics and Automation*, vol. 16, no. 6, pp. 652–662, 2000.